Antonio C. Cancio * and C. Y. Fong
*Department of Physics, University of California, Davis, CA 95616*

J. S. Nelson
*Semiconductor Physics Division, Sandia National Laboratories, Albuquerque, NM 87185-5800*
(Submitted to Physical Review A)

We have studied the exchange-correlation hole $n_{xc}$ and pair correlation function in the valence shell of the Si atom in its $^3$P ground state, using highly accurate Slater-Jastrow wavefunctions and the Variational Monte Carlo method. The exchange-correlation hole shows a number of interesting features caused by the open shell structure of Si, including a marked transition from efficient to poor screening behavior as a test majority-spin electron is moved from the center of a valence $p$ orbital onto the axis perpendicular to the occupied $p$ orbitals. This behavior results from the dramatic difference in the exchange hole in the two cases, which is partially compensated by a corresponding anisotropy in the correlation hole. In addition we observe an anisotropic change in the spin density induced by Coulomb correlation, reducing the spatial overlap between the different spin-components of the density and contributing to the anisotropy of the correlation hole. The exclusion effect correlation, in which a $3s^2 \rightarrow 3p^2$ substitution excitation is allowed along the unoccupied axis and prohibited along the other axes, was found to have a noticeable effect on the correlation hole and is partially accountable for its anisotropy; however, it is inconsistent with the observed changes in spin density. In contrast to the longer range features, we find that the "on-top" correlation hole is well described by linear density functional theory, for a large range of local density and magnetization.

PACS numbers: 31.25.Eb, 31.10.+z, 71.15.-m, 02.70.Lq

## I. INTRODUCTION

An understanding of the exchange-correlation hole and related quantities such as the pair correlation function and exchange-correlation energy is an important factor in the systematic development of accurate density functional theory (DFT) methods for quantum chemistry and solid state physics [1]. Much progress has been made in understanding the pair correlation function in the homogeneous electron gas or jellium, using accurate numerical techniques [2,3] and analytic modeling [4]. Although the closely related Coulomb hole has long been studied in atomic and molecular systems [5–7], the quantitative understanding of correlation holes in inhomogeneous systems is far from complete. In recent years there have been several efforts to fill the gaps, with a focus on characterizing properties closely tied to the development of density functional theories, such as the on-top hole [8,9] and system-averaged exchange and correlation holes [8,10].

In much of the previous work on the exchange-correlation hole in atoms and molecules, the focus has been on two electron systems and closed-shell atoms such as Be and Ne, with additional studies of more complicated molecules such as $N_2$ and $H_2O$ [7]. One class of systems that has received less attention is that of open-shell atoms. The valence shell of such an atom may consist only of a few electrons about a radially symmetric core, but with a degenerate ground state and the corresponding valence-shell structure, have interesting and quite complex features in its exchange-correlation hole. In particular, in the case of less-than-half filling, these include the exclusion-effect correlations involving three or more electrons [11]. Modeling such systems requires proper attention both to orbital correlations best treated in a configuration interaction (CI) context and to dynamic correlations more amenable to a density functional description. The application of density functional theory to open-shell systems is an active area of research, with the question of the optimal treatment of degenerate ground states and of the formation of such atoms into molecules giving rise to intriguing problems [12].

Recently, Variational Monte Carlo (VMC) methods combining highly accurate trial wavefunctions with Monte Carlo methods for evaluating ground state energies and wavefunctions have been developed and applied to atoms and molecules [13–15]. The wavefunctions used in these calculations have the advantage of being simple and compact, typically recovering 85% or more of the correlation energy of atoms and the dissociation energies of molecules with a few trial parameters. Unlike configuration interaction expansions they can describe with equal ease both "nondynamic" correlations and "dynamic" correlations such as the short-range cusp condition [16]. These features make this method a natural candidate for studying electron correlations, and it has been employed in recent studies of the pair correlation function in crystalline Si [17,18].

In this paper we study the exchange-correlation hole

and pair correlation function of the valence shell of the Si atom with the VMC method. A quantitative knowledge of correlations in Si is important in improving DFT predictions for the cohesive energy, binding energies and surface characteristics for this and related technologically important materials. The Si atom is in its own right a useful laboratory for the study of electron correlations, with both local jellium-like and the nonlocal chemical properties due to the open shell structure of the atom playing important roles in determining the relevant physical and chemical properties. The paper is organized as follows: Sec. II provides theoretical background on the exchange-correlation hole, Sec. III gives details of the system studied and of the calculational method. Results for the exchange-correlation hole are given in Sec. IV, for the pair correlation function in Sec. V and for correlation effects on the spin density in Sec. VI. We close with a summary of the results and conclusion in Sec. VII.

## II. THE EXCHANGE CORRELATION HOLE

The exchange-correlation hole, including explicit spin dependence, is defined as:

$$n_{xc}(\mathbf{r}_0,\sigma_0;\mathbf{r},\sigma) = \frac{n^{(2)}(\mathbf{r}_0,\sigma_0;\mathbf{r},\sigma)}{n(\mathbf{r}_0,\sigma_0)} - n(\mathbf{r},\sigma). \qquad (1)$$

Physically it describes the change in density at $\mathbf{r}$ and for spin component $\sigma$ from its mean value, $n(\mathbf{r},\sigma)$, given the presence of another electron with spin $\sigma_0$ at position $\mathbf{r}_0$. The quantity $n^{(2)}(\mathbf{r}_0,\sigma_0;\mathbf{r},\sigma)$ is the pair density, the expectation in the ground state of finding a pair of electrons at two given coordinates. It is defined in terms of an expectation of the ground state as:

$$n^{(2)}(\mathbf{r}_0,\sigma_0;\mathbf{r},\sigma) = \sum_{i,j\neq i} \langle \delta(\mathbf{r}_0-\mathbf{r}_i)\delta_{\sigma_0\sigma_i}\delta(\mathbf{r}-\mathbf{r}_j)\delta_{\sigma\sigma_j}\rangle. \qquad (2)$$

A closely related quantity, the pair correlation function $g(\mathbf{r}_0,\sigma_0,\mathbf{r},\sigma)$, is a measure of the pair density relative to that expected for uncorrelated electrons with the same density distribution:

$$g(\mathbf{r}_0,\sigma_0;\mathbf{r},\sigma) = \frac{n^{(2)}(\mathbf{r}_0,\sigma_0;\mathbf{r},\sigma)}{n(\mathbf{r}_0,\sigma_0)n(\mathbf{r},\sigma)}. \qquad (3)$$

The importance of the exchange-correlation hole to density functional theory lies in its connection [19,20] to the exchange-correlation energy $E_{xc}$:

$$E_{xc} = \frac{1}{2}\int d^3r\, n(\mathbf{r}) \int d^3r' \int_0^1 d\lambda\, \frac{n_{xc}(\mathbf{r},\mathbf{r}',\lambda)}{|\mathbf{r}-\mathbf{r}'|}. \qquad (4)$$

Here $n_{xc}(\mathbf{r},\mathbf{r}',\lambda)$ is the exchange-correlation hole, summed over spins, for the system with scaled Coulomb interaction $\lambda e^2$, with an external potential altered so that the density of the system remains unchanged. The integration over coupling constant strength $\lambda$ accounts for the kinetic energy cost of correlating electrons, weakening the strength of the integrated $n_{xc}$ with respect to its value at $\lambda=1$. Although $E_{xc}$ is in principle determined from a knowledge of the single particle density alone, this dependence is in general not easy to determine beyond the local density approximation. The exchange-correlation hole has a wealth of features which may be used to test and improve theoretical models of the exchange-correlation energy. As a result, many attempts to systematically improve density functional theory have this function as a starting point [1,21–23].

In this paper, we will discuss the full coupling-constant ($\lambda=1$) case for $n_{xc}$. Although the coupling-constant integrated quantity is most directly connected to the density functional theory, the full coupling-constant case is interesting in itself, as its average is an experimentally measurable expectation of the ground state [24]. It is also an essential ingredient in modern hybrid methods which combine elements of density functional theories and conventional Hartree-Fock methods [22]. The quantity $n_{xc}$ is often analyzed by a decomposition into an exchange component, $n_x$, corresponding to the $\lambda = 0$ or noninteracting system, which describes the correlations between particles arising from the Pauli exclusion principle, and a correlation component, $n_c$, determined by taking the difference between the fully interacting and noninteracting cases, which describes the additional correlation due to the Coulomb interaction between electrons [25]. We study the explicit spin decomposition of $n_{xc}$. This choice is useful for understanding the correlation response of an open-shell atom for which the ground state has nontrivial differences in its spin components. Spin decomposition falls roughly along the lines of exchange and correlation: exchange affects only particles with the same spin, and Coulomb correlations, though also present in the same-spin case, are most noticeable in the opposite-spin channel.

Some initial insight into the nature of the exchange-correlation hole in atoms and other finite systems can be obtained by considering limiting cases. The exchange-correlation hole about a reference electron in the homogeneous electron gas is isotropic, that is, a function solely of the distance from the electron, and localized about the electron with a radius determined by the average interelectron distance. Consequently, in a system of slowly varying density, the the local density approximation (LDA) holds, in which the hole is determined by the density (or each spin-component of the density if these are different) at the location of the reference electron and "moves" with the position of the reference electron. In atoms or molecules, important correlation effects often involve a pair excitation from the noninteracting ground-state into a finite number of lowlying, perhaps nearly degenerate, excited states. In this case, the resulting correlation hole is dependent on the shape of the ground-state orbitals vacated and the excited-state orbitals occupied

and is largely unsensitive to the position of the reference electron. In real systems, the exchange-correlation hole will contain aspects of both limiting cases, with those that "move" with the position of the electron termed "dynamic" correlations and the orbital correlations insensitive to electron position termed "nondynamic". In open-shell atoms both play important roles.

## III. CALCULATION APPROACH

### A. Correlated description of the Si atom

We focus on correlations in the valence shell of the atom with the core electrons replaced by norm-conserving *ab initio* nonlocal pseudopotentials derived from LDA calculations [26]. In this case the valence shell of the atom is described by the Hamiltonian

$$H = \sum_i \left( \frac{\nabla_i^2}{2m} + \sum_{l_i,m_i} V_{l_i}(r_i)|l_i m_i><l_i m_i| \right) + \sum_{i<j} \frac{e^2}{|\mathbf{r_i} - \mathbf{r_j}|} \quad (5)$$

where the sums are over the valence electrons. $V_l$ is the nonlocal pseudopotential and $|l_i m_i >< l_i m_i|$ the single particle projection operator onto the state with total angular momentum $l_i$ and $z$-axis projection $m_i$. The final term is the intravalence Coulomb interaction.

The Si atom has a nine-fold degenerate $(3s^2 3p^2)$ $^3P$ ground state. By maximizing the spin projection, this state can be represented by a single Slater determinant, consisting of a majority-spin component, here chosen to be spin up, with one $3s$ and two $3p$ orbitals, and a minority or down-spin component with one $3s$ electron. There then remain two angular momentum projections that lead to physically significant differences in $n_{xc}$. The $m_l = 0$ projection has $p_x$ and $p_y$ orbitals and a "pancake" like shape, while the $m_l = \pm 1$ projections have a "cigar" shape, with $p_0$ and $p_\pm$ orbitals. This distinction does not play a role in determining $E_{xc}$ for an atom, given the invariance of the energy to rotations of the atom. The presence of a quantization axis in the formation of a Si bond breaks this invariance, so that the projection-specific behavior of $n_{xc}$ becomes important in determining accurate molecular binding energies. It thus should be useful as a test of density functional theory, which typically overestimates binding energies by about 1 eV [1,10]. Results in this paper focus on the $m_l = 0$ projection which provides a clear comparison between the situation perpendicular to and parallel to the $p$ orbitals, though calculations were done on the other projection for comparison.

To calculate the exchange-correlation hole variationally we start with a Slater-Jastrow trial wavefunction

$$\psi = exp(-F) \prod_\sigma D_\sigma, \quad (6)$$

with $D_\sigma$ being a Slater determinant for spin component $\sigma$ and $F$ a Jastrow correlation factor. All single-particle orbitals are obtained from the same local DFT program that determined our pseudopotentials. We use a Boys and Handy form [14,27] for $F$, which includes electron-electron, electron-nucleus and electron-electron-nucleus correlations expanded in a basis set of correlation functions:

$$F = \sum_{l,m,n} c_{lmn} \sum_{i \neq j} (\bar{r}_i^l \bar{r}_j^m + \bar{r}_i^m \bar{r}_i^l) \bar{r}_{ij}^n. \quad (7)$$

The basis functions are $\bar{r}_i = br_i/(1 + br_i)$ and $\bar{r}_{ij} = dr_{ij}/(1 + dr_{ij})$, where $r_{ij}$ is the distance between a pair of electrons, $r_i$ is the distance between electron $i$ and the atom center. The terms $b$, $d$ and $c_{lmn}$ are variational parameters. The lowest order $\bar{r}_{ij}$ term is set separately for opposite and same-spin electron correlations to satisfy the short range electron-electron cusp condition [16] for each case. Higher order terms treat longer range effects and are determined without distinguishing electron spin. Electron-ion terms in the correlation function correct for the tendency of interelectron correlations to expand the volume of the atom and provide density-dependent corrections to the electron-electron correlation [14]. Since the valence shell of Si is less than half-filled, orbital or nondynamic correlations may be important [11]. These can be incorporated with a multideterminant extension of the Slater-Jastrow wavefunction:

$$\psi = exp(-F) \sum_\alpha \eta_\alpha \prod_\sigma D_\sigma^\alpha. \quad (8)$$

### B. Method of Calculation

The Variational Monte Carlo method [28] is used to calculate the ground-state energy, derivatives with respect to variational parameters, and other expectation values. The heart of the method lies in the judicious statistical sampling of integration points to obtain an estimate of the many-body integrals involved in evaluating expectations of the Slater-Jastrow trial wavefunction. This estimate is limited in accuracy by statistical noise; however if the trial wavefunction is a good approximation to the ground-state wavefunction this noise can be very easily managed with a relatively small number of configurations [13]. Optimized wavefunctions are obtained by minimizing the variance of the energy [13]. With a trial wavefunction of 18 expansion terms including two set by the same- and opposite- spin cusp conditions, up to $l+m+n = 6$ in the basis function expansion, we obtain a value of 3.8028(2) a.u. for the ground-state valence-shell energy. The correlation energy, measured with respect to a noninteracting ground-state energy of 3.7188 a.u., is 97% of the correlation energy obtained from Green's function Monte Carlo and 95% of that obtained from CI

using the same nonlocal pseudopotential [15]. A similar calculation starting from a two determinant reference point [Eq. (8)], adding the $3p_z^2 3p_x 3p_y$ excited state to the noninteracting ground-state configuration, resulted in a modest improvement in energy to 3.8041(2) a.u. or 96.6% of the valence-shell correlation energy with respect to CI.

To calculate correlation functions, we measure spin-decomposed single-particle densities $n(\mathbf{r},\sigma)$ and conditional densities $n(\mathbf{r},\sigma|\mathbf{r}_0,\sigma_0)$. The spin-dependent conditional density is defined as the ground-state density distribution as a function of spin $\sigma$ and position $\mathbf{r}$ of the $N-1$ other particles given one with spin $\sigma_0$ fixed at $\mathbf{r_0}$. The difference between the conditional and "unrestricted" densities, gives the spin-dependent exchange-correlation hole, Eq. (1),

$$n_{xc}(\mathbf{r_0},\sigma_0;\mathbf{r},\sigma) = n(\mathbf{r},\sigma|\mathbf{r}_0,\sigma_0) - n(\mathbf{r},\sigma). \qquad (9)$$

Separate calculations are done to measure the density and the conditional density for various values of $\mathbf{r_0}$ and $\sigma_0$. These expectations are first calculated exactly for the Slater-determinant wavefunction (setting $F=0$ in our trial wavefunction). Then, the difference between the expectations obtained with the Slater determinant and the fully interacting wavefunctions is measured statistically using Monte Carlo sampling and the method of correlated estimates [28]. This technique is an efficient means to estimate statistically the change in the expectation of an observable under a small perturbation of the Hamiltonian or of the variational parameters of the wavefunction, taking advantage of the high degree of correlation between the two expectations to reduce noise in the difference of their statistical estimates. In the present case, the correlation hole, which describes the difference between the correlated and Slater-determinant exchange-correlation holes, is fairly small compared to the exchange-correlation hole. It is thus a reasonable assumption that the correlated estimation approach should improve the sampling efficiency for this quantity. In practice, the procedure was observed to reduce statistical errors in our data by a factor of 5, and roughly $10^5$ random samples of the wavefunction sufficed to obtain expectation values.

The expectations for density and conditional density were expanded in a plane wave basis, taking the average of $\sum_i exp(-i\mathbf{G}\cdot\mathbf{r}_i)$ for a set of plane waves up to a 32 Ry cutoff, on a supercell 18 Bohr radii ($a_B$) in length. The coefficients were symmetrized and fast-Fourier transformed to obtain real-space densities. This expansion provides smooth profiles despite the statistical noise of the sampling. On the other hand the short-wavelength cutoff causes an unrealistic rounding off of the correlation hole cusp at short interparticle distances, and spurious oscillations at low densities. At present this cutoff is the largest error in our calculation. In the case of the exchange-correlation hole this error is notable mostly in the cusp region. A more complete discussion of errors is presented in Sec. V in regard to the pair correlation function which is more sensitive to the cutoff error than the exchange-correlation hole.

## IV. RESULTS FOR THE EXCHANGE-CORRELATION HOLE

The exchange hole in DFT is obtained by evaluating $n_{xc}$ from Eq. (1) for the Slater determinant wavefunction that minimizes the energy in the noninteracting ($\lambda=0$) limit: with the Coulomb interaction replaced by a single-particle potential that reproduces the true ground-state density [20]. In practice the Slater determinant of local DFT orbitals used in our calculations produces a density that differs from our VMC density by a few percent. In terms of these orbitals, the exchange hole is:

$$n_x(\mathbf{r}_0,\sigma_0;\mathbf{r},\sigma) = \frac{-\left|\sum_{\alpha=1}^{N_\sigma}\psi_\alpha^*(\mathbf{r}_0,\sigma)\psi_\alpha(\mathbf{r},\sigma)\right|^2\delta_{\sigma\sigma_0}}{n(\mathbf{r}_0,\sigma_0)} \qquad (10)$$

where the sum runs over all the occupied single-particle orbitals $\psi_\alpha$ for the spin component $\sigma$. This expression, as a function of $\mathbf{r}$ for fixed $\mathbf{r}_0$ (*i.e.*, interpreting the hole as the change in density of the system at $\mathbf{r}$ given a particle observed at $\mathbf{r_0}$) has the form of minus the probability density of a hybrid atomic orbital. That is, it describes a normalized linear combination of single-particle orbitals with coefficients $c_\alpha = \psi_\alpha^*(\mathbf{r}_0,\sigma_0)/\sqrt{n(\mathbf{r}_0,\sigma_0)}$. This choice of $c_\alpha$ for each orbital $\psi_\alpha$ represents the unique linear combination of orbitals that maximizes the probability for an electron to be observed at $\mathbf{r_0}$ and spin $\sigma_0$ (conversely giving zero likelihood for any other electron to be observed at that point.) Finally the integral over $\mathbf{r}$ of the exchange hole is $-1$, as it measures the integrated difference in density between the $(N-1)$-electron system given one electron fixed at $\mathbf{r_0}$ and the full $N$-electron system.

For a spin-up particle on the $z$ axis in the $L_z=0$ projection, this exchange-hole orbital is a $3s$ state since the occupied $p$ states ($p_x$,$p_y$) are in the $x$-$y$ plane. The exchange hole is completely insensitive to the electron position on this axis, given only one possible orbital from which to construct it. The situation along this axis thus corresponds to an extreme departure from the "dynamic" picture of the exchange hole derived from the homogeneous electron gas. For a particle on the $x$ axis, the hole is a combination of $s$ and $p_x$ orbitals. We find that the occupation probability $|c_p|^2$ of the $p$ orbital to be between 60% and 75% in the region ($0.5\ a_B < x < 2.5\ a_B$) of peak density along the $x$ axis; this is roughly equivalent to that of a $sp^2$ hybrid orbital (which is two-thirds $p$) oriented in the direction of the fixed particle. The slight variation in the $c_p$ acts to keep the hole more or less centered on the reference electron in the region of peak density on the $x$-$y$ plane. The exchange hole as a result is more sensitive to the exact location of particles in this plane, and therefore more efficient in screening them, than along the $z$ axis, leading to significant differences in the correlation

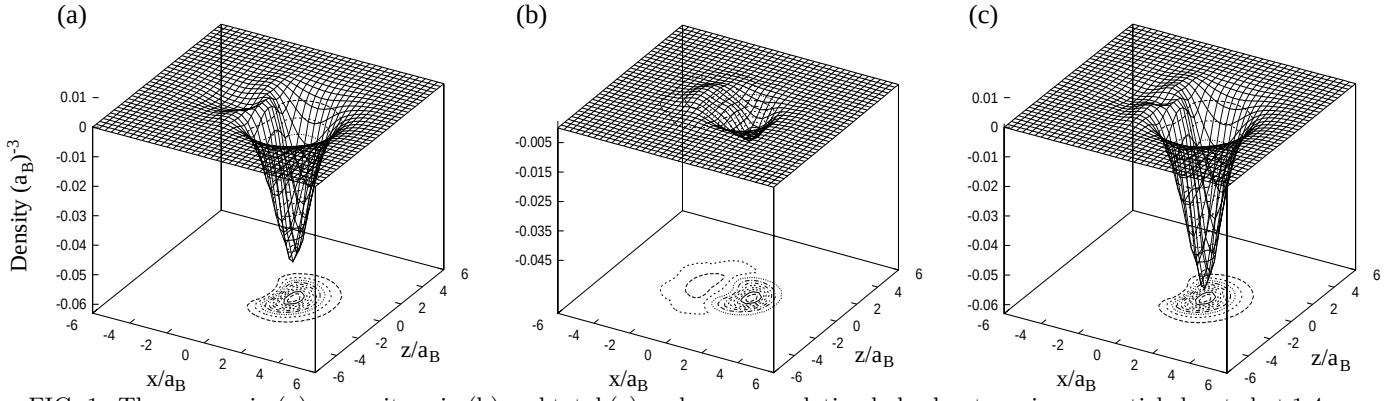


FIG. 1. The same spin (a), opposite spin (b) and total (c) exchange-correlation hole about a spin-up particle located at 1.4 $a_B$ from the atom center on the $x$ axis (parallel to the $p$ orbitals) for the ground state of the Si atom in the $L_z = 0$ projection. The surface plot shows the change in density along a plane cutting through the origin along the $x$ and $z$ axes.

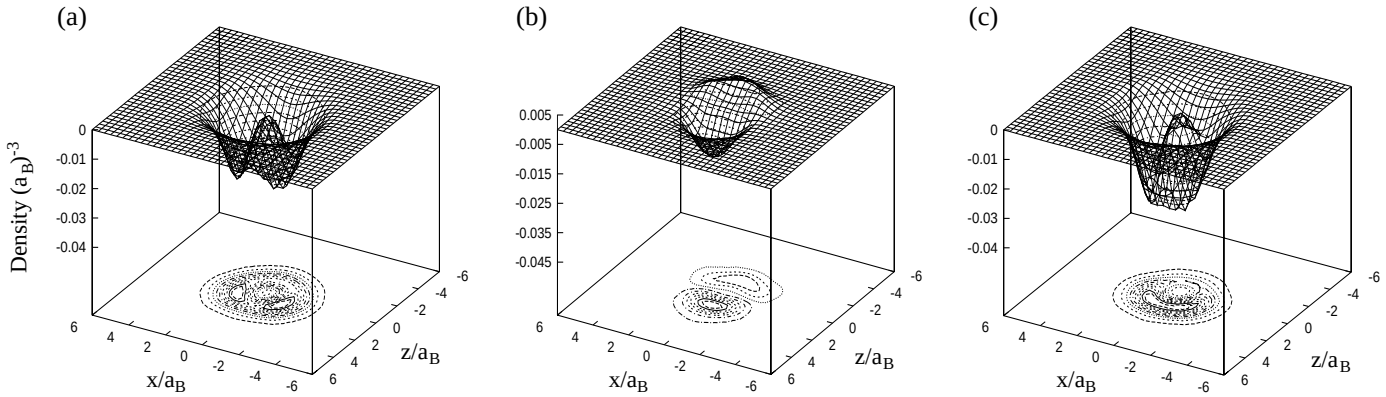


FIG. 2. The same spin (a), opposite spin (b) and total (c) exchange-correlation hole about a spin-up particle located at 1.4 $a_B$ from the atom center on the $z$ axis (perpendicular to the $p$ orbitals). Cut through atom as in Fig. 1.

holes in the two cases as well. This transition from "non-dynamic" screening along the axis perpendicular to the occupied $p$ orbitals to a more "dynamic" screening in the plane occupied by them, particularly as it occurs at peak density in the valence shell, constitutes a major difference between the $n_{xc}$ of Si and that of closed-shell atoms.

In Figs. 1 and 2 we plot the exchange-correlation hole about a spin-up electron fixed at the point of peak density parallel to and perpendicular to the two $3p$ orbitals of the $m_l = 0$ (pancake) projection of the Si atom. The single-configuration Slater-Jastrow wavefunction [Eq. (6)] is used. Each plot shows the response to this electron in the $x$-$z$ plane, that is, the plane cutting through the center of the atom at the plot origin, with one axis ($x$) parallel to and one ($z$) perpendicular to the occupied $p$ orbitals. The hole is split into same spin (a), opposite spin (b) and total (c) response. The comparison between these two situations shows the dramatic anisotropy in $n_{xc}$ reflecting that of the exchange hole.

For a spin-up electron placed on the $x$ axis, Fig. 1, the exchange-correlation hole is dominated by the $sp^2$-like exchange hole. The additional effects of Coulomb correlation on the same-spin channel are hard to detect, while the opposite-spin correlation hole is small (contributing 14% of the total on-top hole, or value of the hole at zero interparticle separation.) It is largely confined to a narrow region about the electron, indicating that the $sp^2$ hybrid hole screens the electron efficiently.

Fig. 2 shows the exchange-correlation hole of a spin-up electron on the $z$ axis, perpendicular to the two $p$ orbitals. With the addition of correlation, the same-spin hole (a) loses the rotational symmetry of the $3s$ state that characterizes the exchange hole, with the polarization of the two $3p$ orbitals creating a double valley on either side of the reference electron. The opposite-spin hole (b) shows the polarization of the $3s$ spin-down orbital, with a well centered about the fixed electron and a strong dipole response at longer range.

The total $z$-axis exchange-correlation hole, (c), shows a smooth interpolation of the two spin contributions leading to a large crescent-shaped area near the electron from which the other electrons are repelled. The correlation hole contributes considerably to the total exchange-correlation hole, with up to 40% of the total on-top hole due to correlation. Although the $3s$-orbital exchange hole is highly nonlocal and does not efficiently screen the electron, the correlation contribution goes a long way to make the total hole more local.

In addition to the obvious differences in $n_{xc}$ along each axis due to the differences in the exchange hole, Figs. 1 and 2 reveal subtle differences in the opposite-spin hole. The extent of the orientational anisotropy in the opposite-spin hole can be better visualized by plotting the hole along the $x$ axis for the up-spin electron fixed on the $x$ axis and along the $z$ axis for the electron fixed on the $z$ axis, cutting through the minima and maxima of the contour plots Figs. 1(b) and 2(b). These are represented as solid lines in Figs. 3(a) and (b). The most notable difference between the two cases is the height of the peak on the side of the atom opposite the reference electron, which is three times as large along the $z$ axis (b) as on the $x$ axis (a). In addition the minimum is slightly deeper for the $z$-axis case.

Additionally, in Figs. 3(a) and (b) we show trends in the opposite-spin correlation hole as one gradually removes the reference electron from the atom. In addition to the 1.4 $a_B$ case discussed above, we place a spin-up electron on the $x$ axis (a) and the $z$ axis (b), at a distance of 2.0 and 4.0 $a_B$ from atom center, and plot the on-axis response of the spin-down electron as long- and short-dashed lines respectively. These three reference radii correspond to placing an electron at the peak valence density along either axis, at the average radius from the atom, and at a low density point outside the atom respectively. As the electron is moved to lower densities, the shape of the minimum slowly gets wider and shallower, consistent with trends in the homogeneous electron gas. The position of the hole minimum stays near the atom, and thus increasingly more off center with respect to the electron. This is expected: the correlation hole, measuring the change in density in the presence of an electron at some reference point, can have an absolute value no greater than the density itself. Along the $x$ axis, this trend to a shallow off-centered hole is correlated with a gradual increase of peak height on opposite side of atom. For the $z$-axis case the peak height remains roughly constant as the electron is removed.

It is interesting to compare these results to recent analytic studies of the asymptotic limit of the exchange-correlation hole of Be and Ne [8,29]. In the limit of an electron far removed from the atom, $n_{xc}$ measures the collapse of the remaining $N-1$ electrons to an eigenstate of the positive ion. The correlation component of $n_{xc}$ measures the change in electron density due to the reduced Coulomb reduction between the remaining electrons. At intermediate distances, a few atomic radii from the atom center, $n_{xc}$ also shows a dipole polarization of the atom, or a reduction of electron density from the side of the atom nearer the reference electron to the farther side, more so for the more polarizable Be than for Ne. The collapse to the ion in the asymptotic limit results in a correlation hole peaked in the center with a minimum around the edge of the atom. This may possibly be seen in our data for the 4.0 $a_B$ $x$-axis case of Fig. 3(a), where the correlation-hole profile develops a peak on both sides of the ion core. The correlation hole along both axes

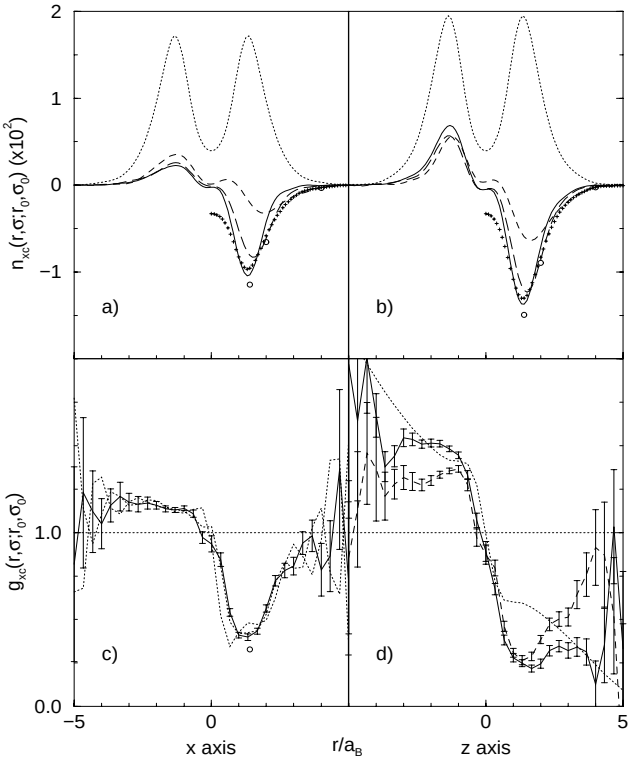


FIG. 3. Spin-down response to a spin-up electron: (a) the correlation hole along the $x$ axis for a spin-up electron fixed on the $x$ axis at positions 1.4 (solid line), 2.0 (long-dashed) and 4.0 $a_B$ (dashed line) from the atom origin. (b) the correlation hole along the $z$ axis for an electron fixed at corresponding positions on the $z$ axis. (c) the pair correlation function for the 1.4 $a_B$ case of (a), for energy cutoff of 20, 28 (both dotted lines) and 32 Ry (solid line). (d) the pair correlation function for the 1.4 $a_B$ case of (b) for three trial wavefunctions: $\psi_{S-J}$ (dashed line), $\psi_{CI}$ (dotted), $\psi_{CI-J}$ (solid line). In (a) and (b), the mean spin-down density is plotted for comparison as a dotted line. Additionally, the circles show the value for the "on-top" hole for each case plotted and the crosses, the LSD on-top hole for various points along each axis. Error bars show the standard deviation of the VMC expectation measured over several statistically independent runs.

shows evidence of a dipole polarization of the valence shell when the reference electron is moved outside the atom, with a larger response on the "Be-like" $z$ axis than along the "Ne-like" $x$ axis. The contrast between Si and closed-shell atoms is that this polarization of the valence shell does not die out when a reference electron on the $z$ axis is moved into the center of the valence shell, if anything becoming more pronounced, while the polarization is damped out along the $x$ axis under the same circumstances. An added complexity for Si is that the final state of the system after removing an up-spin electron in different directions corresponds to different atomic configurations: $3s3p^2$ for the $z$-axis case (removal of the up-spin $3s$ orbital) but $3s^23p$ for the $x$ axis. Thus significant differences between the correlation and exchange holes induced by electrons on different axes remain even for

electrons asymptotically far from the atom.

We have also studied the local features of the exchange-correlation holes plotted, especially the opposite-spin on-top correlation hole, $n_{xc}(\mathbf{r},\sigma;\mathbf{r},-\sigma)$. This measures the reduction in the opposite-spin electron density at the location of a given electron. As the correlation hole is deepest when the Coulomb repulsion is largest, the on-top hole also represents the lower bound for the correlation hole at any position in the atom [30]. In previous papers, it was observed that this feature was well described in several small atoms [8,9] and in Hooke's atom [31] by a local spin-density (LSD) ansatz, using the on-top hole of the homogeneous electron gas corresponding to the density and magnetization at the location of the electron pair:

$$n_{xc}^{LSD}(\mathbf{r},\mathbf{r}) = n(\mathbf{r})(g^{heg}(0,n(\mathbf{r}),\zeta(\mathbf{r}))-1). \qquad (11)$$

Here $g^{heg}(u,n,\zeta)$ is the pair correlation function of the homogeneous electron gas at density $n$, magnetization $\zeta=(n_\uparrow-n_\downarrow)/n$, and interparticle separation $u$. In this sense, it represents a link between the homogeneous electron gas and dynamic correlations in many inhomogeneous systems [32].

In Figs. 3(a) and (b) we plot the LSD on-top hole, using homogeneous electron gas values from Ref. [33], at each point along the $x$ and $z$ axes (crosses). These are compared to on-top holes of the Slater-Jastrow wavefunction [Eq. (6)] evaluated specifically at the location of the electron for the correlation holes shown (circles at 1.4, 2.0, and 4.0 $a_B$). These values for the Slater-Jastrow on-top hole are calculated directly without recourse to a plane-wave expansion, using VMC with a constrained pair random walk [34], and are exact within a negligible statistical error. The finite energy cutoffs employed for the rest of the data tend to lose sharp features of the correlation hole, in particular that of the cusp condition at zero interparticle separation. The resulting disagreement with the exact (for the trial wavefunction used) values is at worst 20% and usually better. The LSD model agrees fairly well with the VMC data, within $10-20\%$ for most of the points calculated here, faithfully following the observed trends with respect to electron position. It provides a fairly reasonable lower limit for the correlation hole at all points in the atom. A calculation of the on-top hole about the spin-down electron was also done, with similar agreement with theory.

It is interesting to consider in further detail the anisotropy in the opposite-spin contribution to $n_{xc}$ at peak density. In the cases shown in Figs. 1-3, it can be interpreted as the measure of the polarization of the down-spin electron density in the presence of an up-spin electron. At first glance, one might guess that this down-spin polarization should roughly be invariant with respect to the angular orientation of the up-spin electron since one is measuring the response of the down-spin $s$-orbital to the angle-independent Coulomb interaction. More precisely, one measures the correlations induced by the optimized Jastrow factor which depend only on interelectron and electron-nucleus distances. The difference in the opposite-spin holes Figs. 1(b) and 2(b), is thus a direct reflection of the influence of the determinantal structure of the three up-spin electrons on the correlation response of the down-spin one.

In the LDA, the influence of the environment on interparticle correlation is modeled by the variation with local density of the correlation hole, taken to be that of the homogeneous electron gas [3,4] at the local density. Typically the largest absolute and relative effects in this model are felt at the on-top hole. At this point it seems to describe the observed behavior quite well, with the variation in density going from the maximum of the $p$ orbital on the $x$ axis to the open $z$ axis accounting for the difference in the peak density on-top holes. However, the large discrepancy between the maxima of the peak density $z$-axis and $x$-axis hole, the solid lines in Fig. 3a and 3b, as well as their relatively large size, is inconsistent with this model. Neither does it seem easily explained by local gradient corrections, as the two points are located at a density maximum and a saddle point respectively, where any correction would be only second order in the gradient and therefore quite small.

Within the context of a variational wavefunction calculation, a mechanism that can introduce an orientation dependence into the correlation hole of an open shell atom is the three-electron "exclusion effect" or Fermi correlation [11] in configuration-interaction theory, which should be observable for second row atoms with less than half filling in the $3p$ valence shell. For Si in the $L_z=0$ projection considered here, there is a "nondynamic" contribution to the correlation between electrons along the $z$ axis due to a $3s^2$ to $3p_z^2$ excitation that is forbidden for the corresponding $x$- or $y$-axis analogs by Pauli exclusion. This contribution to the correlation hole about an up-spin electron on the $z$ or "unoccupied" axis, and the absence of the same about one on "occupied" axes leads to a difference in the holes observed with reference points on these axes. Since this particular configuration is within the $3p$ valence shell, and thus fairly close to the ground state energy, it is natural to expect it to play a significant role in the observed difference in response.

What is striking here is that the observed orientational dependence of $n_{xc}$ is obtained with a single Slater-determinant configuration modified by a Jastrow factor that depends only on interparticle distance and the distance of particles from the core. There are no explicit orbital correlations in this trial wavefunction [Eq. (6)]. The Slater-Jastrow wavefunction, coupling a Jastrow factor with a determinant formed from an incomplete set of valence orbitals, in principle could have a nonzero overlap with the $3p_z^2 3p_x 3p_y$ configuration allowed in the normal exclusion-effect model, and no overlap with the excluded excitations. However, this would be only one of an infinite number of configurations implicitly included in the Slater-Jastrow wavefunction, tied together by a "dynamic" correlation factor that gives no particular varia-

tional weight to any one configuration. Thus it is unlikely that it would fully account for the observed differences in the response along the occupied and open axes [35].

On the other hand, a more general argument involving screening can be invoked to explain the orientational anisotropy in our results. If the up-spin electron is placed on the $z$-axis, its exchange hole is not centered on the electron position, as the electron occupies a $3s$ orbital with an isotropic spatial extension throughout the atom's valence shell. The net effect of the electron plus its exchange hole has the nature of a dipole field along the $z$ axis of the atom, with an imperfectly screened negative charge on the side of the atom nearest the electron and a positively charged region due to the exchange hole on the other side. The large peak in the down spin electron's response to the up-spin electron can be viewed then as a dipole induced by the dipole field formed by the imperfect exchange screening of the up-spin electron. In the $x$-axis case, the exchange hole is centered and localized on the electron; the other two electrons are in $sp^2$ orbitals blocking out the rest of the valence shell. Therefore the up-spin electron is efficiently screened by its exchange hole, and in addition, there is no "easy" direction for redistributing the down-spin electron density. In such a picture the $3s^2 \rightarrow 3p^2$ excitation should play an important but not exclusive role in the overall dipole response along the $z$ axis. This effect is observable in a Slater-Jastrow wavefunction because the Jastrow factor includes correlations simultaneously between all particle pairs. Thus, the correlation response of the down-spin electron to a fixed up-spin electron involves not only their mutual Coulomb repulsion but that of the other up-spin electrons as well. The inhomogeneous distribution of these electrons about the fixed electron combined with the effect of the external potential in essence create a Coulomb interaction with the exchange hole.

## V. RESULTS FOR THE PAIR CORRELATION FUNCTION

### A. Single Configuration Wavefunction

In a system such as an atom, the pair correlation function $g(\mathbf{r_0}, \sigma_0; \mathbf{r}, \sigma)$ is a valuable tool because, given the large variation in the density over the length-scale of the exchange-correlation hole, the shape of the hole is to a large extent determined by the variation in density. The pair correlation function can distinguish the intrinsic effects of correlation by eliminating any features that are simply proportional to the density.

In Fig. 4 we plot the pair correlation function (PCF) for several of the cases considered previously. Specifically, we show $g(\mathbf{r_0}, \uparrow; \mathbf{r}, \downarrow)$ fixing a spin-up particle at the peak in the valence density, 1.4 $a_B$ on the $x$ axis (a) and the $z$ axis (b) and plotting the variation with respect to the spin-down electron in the $x$-$z$ plane. These results are obtained by dividing $n_{xc}$ as plotted in Figs. 1(b) and 2(b) respectively by the spin-down density, with a constant shift of 1 due to the differing conventions in their definitions [Eqs. (1) and (3)]. The value $g = 1$ corresponding to $n_{xc} = 0$ (shown as a thick contour in Fig. 4) denotes the boundary between the region in which the spin-down density has been reduced ($g < 1$) and that in which it has been enhanced ($g > 1$) in the presence of the spin-up reference electron. As described in the next section the PCF can be significantly affected by statistical error at low density, so that the plot range is restricted to higher density regions where the statistical error is less than half a contour increment in either direction.

The contours of the pair correlation function in the vicinity of the spin-up electron on the $x$ axis are nearly circular and centered on the electron, showing the spin-down electron repelled from it without significant directional bias. The $g = 1$ contour is slightly oblong in shape, indicating that at longer distances there is a slight bias towards shifting electron density to the high density areas on the far side of the atom ($x < 0$). A similar plot cutting through the $x$-$y$ plane (ie, cutting through both the $p$ orbitals along a plane perpendicular to the one shown) shows similar results except that the $g = 1$ contour is more circular in shape. This picture is fairly consistent with that of a homogeneous electron gas PCF which depends only on the distance between particles, and indicates that the underlying physical processes are quite similar: high energy "dynamic" correlations that are quickly screened out over the radius of the exchange hole.

In comparison, the PCF in Fig. 4(b), showing the response to the spin-up electron on the $z$ axis shows a much greater departure from isotropy. The function has a noticeable dipole component with respect to the atom center, with a peak in $g$ directly opposite the minimum on the $z$ axis. The $g = 1$ contour has a much more shallow curvature than that of Fig. 4(a), so that it is no longer centered on the spin-up electron, but rather coincides roughly with the $z = 0$ plane in the high density region of the atom. (For the $3s^2 3p_x 3p_y$ configuration of Si, the PCF with a reference electron on the $z$ axis is rotationally invariant about the $z$ axis so that the contours shown in the plot can be extended to surfaces of rotation in three dimensions.) In the near vicinity of the fixed electron, the pair correlation function is no longer a function of the distance between the two coordinates $\mathbf{r}$ and $\mathbf{r_0}$ alone, but has taken on a noticeable angular dependence as well. Thus the slope of the well near 1.4 $a_B$ on the $z$ axis is steeper towards the center of the atom, shallower towards the outer edge of the atom. Although such a shape could in principle be accounted for in a region where the gradient of the density is large, using a gradient expansion of the homogeneous electron gas [36], it cannot be explained along these lines in the current situation since it occurs at local saddle point in the density (the peak of the density along the $z$ axis). These features in the PCF confirm the existence of a genuine directional anisotropy in the response to an electron located perpendicular to

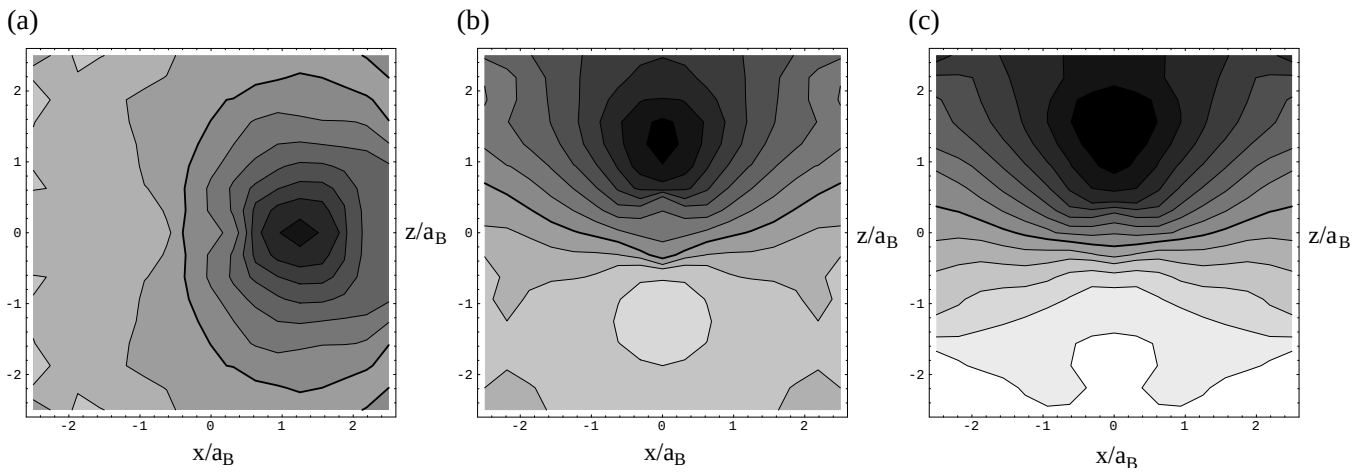


FIG. 4. The opposite-spin pair correlation function $g(\mathbf{r_0}, \uparrow; \mathbf{r}, \downarrow)$ as a function of spin-down electron position in the $x$-$z$ plane for a spin-up particle fixed at (a) 1.4 $a_B$ from the atom center on the $x$ axis, (b) 1.4 $a_B$ from atom center on the $z$ axis, (c) the same as (b), with nondynamic correlations from the $3s^2$ to $3p_z^2$ double substitution included. The contour increment is 0.1 with the contour for $g=1$ represented by a thicker line; the regions between are shaded darker for lower values of $g$.

the occupied $p$ orbitals, and suggest that the explanation lies in a nonlocal mechanism such as the response to a poorly localized $3s$ exchange hole.

Along this line, it is instructive to consider the exchange-correlation hole about the lone down-spin electron. In this case the exchange hole is of necessity due to the $3s$ orbital regardless of the electron position, and one can expect significant departures from a compact, isotropic PCF. In the case of a down-spin electron on the $z$ axis, we observe the PCF that is very close to that about an up-spin electron, with perhaps a slightly larger dipole component. In both cases, the PCF indicates the presence of a significant dipole response that compensates for the poorly screening $3s$ exchange hole. The PCF for a down-spin electron on the $x > 0$ axis has a quite complicated pattern outside the on-top hole region – neither roughly isotropic like Fig. 4(a) or with simple dipole anisotropy like Fig. 4(b). There are several unconnected regions where the electron density is enhanced: surrounding the electron for $x > 0$ and focused on the $x$ axis opposite the electron for $x < 0$. In this case the exchange hole should not screen the electron efficiently, but there is no lowlying $3p$ orbital with which to construct a response, so that there is a possibility that the contributions of higher-order orbitals might be observable.

### B. Two Configuration Wavefunction

Since we have observed a significant change in shape of the opposite-spin PCF with respect the angular orientation of the reference electron, using a single-determinant Slater-Jastrow wavefunction, it is interesting to include explicitly the $3s^2 \rightarrow 3p_z^2$ excitation that is predicted in CI theory to play a prominent role in producing such a behavior in the Si atom. We consider the multideterminant wavefunction $\psi_{CI}$ that consists of a $3p_z^2 3p_x 3p_y$ excited state configuration as well as the noninteracting ground state. This wavefunction can be treated alone or used as a starting point for adding further correlations via the Jastrow factor [Eq. (8)]; in either case the mixing amplitude $\eta_1$ for the excited state is variationally optimized, along with the Jastrow parameters for the latter case. We obtain a mixing coefficient $\eta_1$ of 0.132 and total energy 3.7263(18) a.u. in the former case and 0.056 and 3.8041(2) a.u. in the latter.

The nondynamic correlation modeled by the two-configuration wavefunction alone, $\psi_{CI}$, is to first order in $\eta_1$ a dipole-dipole correlation:

$$g_{CI}(\mathbf{r_0}, \uparrow; \mathbf{r}, \downarrow) = 1 + 2\eta_1 \frac{z_0}{r_0}\frac{z}{r}\frac{R_p(r_0)}{R_s(r_0)}\frac{R_p(r)}{R_s(r)} \qquad (12)$$

where $R_p$ and $R_s$ are the radial $3s$ and $3p$ orbitals. The signature of this PCF in a contour plot with the cut through the $x$-$z$ plane and $r_0$ fixed on the $z$ axis is a series of roughly straight lines arranged antisymmetrically about the $z = 0$ plane, with the $g = 1$ contour at $z = 0$. The shape of the function is independent of the position of the fixed particle, with the only change being in the overall amplitude. For one electron fixed on the $x$ axis, on the node of the $p_z$ orbital, the PCF is to first order zero.

In Fig. 4(c) we show a contour plot for the opposite-spin PCF of the combined CI plus Jastrow wavefunction, $\psi_{CI-J}$, for the same plot parameters as Fig. 4(b): with the up-spin electron fixed at 1.4 $a_B$ on the $z$ axis. In this case the occupation probability of the excited-state Slater-Jastrow wavefunction is very small, 0.3%, and the change in the total ground-state energy from the single-determinant Slater-Jastrow wavefunction is correspondingly small. On the other hand the explicit addition of the nondynamic correlation increases the correlation energy by 1.6% and has a significant impact on the shape

of the hole. The PCF has a clear dipole-dipole signature, exaggerating the spatial anisotropy already visible in the one determinant case. The $g=1$ contour is closer to the $z=0$ axis, and the short-range well about the fixed particle, which for a particle near the peak of the valence shell density could be expected to be fairly deep and isotropic, has been reduced to a shallow and open-ended dip. As expected from the form of the nondynamic correlation, little change was observed in the PCF for a particle fixed on the $x$ axis.

A quantitative comparison of $g$ for the above cases is also instructive and is shown in Figs. 3(c) and (d). We plot $g(\mathbf{r_0}, \uparrow; \mathbf{r}, \downarrow)$ varying $r$ along the $x$ axis and fixing $\mathbf{r}_0$ at 1.4 $a_B$ on the $x$ axis (c) and the analogous situation for the $z$-axis (d). Error bars on the statistical measurements of these quantities are plotted, as well as the plane-wave cutoff dependence for the $x$-axis case. The converged result on the $x$ axis (solid line) is well localized about the reference particle's position, with an enhancement of particle density on the opposite side of the atom.

The results for the $z$ axis, Fig. 3(d) include the PCF for the three different trial wavefunctions discussed above: the single Slater determinant plus Jastrow factor, $\psi_{S-J}$ (dashed line), the two-configuration wavefunction $\psi_{CI}$ (dotted line) and the same multiplied by a Jastrow factor $\psi_{CI-J}$ (solid line). In comparison to the most accurate result, $\psi_{CI-J}$, $\psi_{CI}$ predicts with some success the long-wavelength polarization response to the electron at $\mathbf{r_0}$, determining how much the electron density is pushed from one side of the atom to the other. The major difference is the absence of the small dip in the immediate vicinity of the electron due to the cusp condition, which naturally is not obtained from the two-configuration wavefunction. In contrast, $\psi_{S-J}$, which does not include explicit orbital-dependent correlations but can be optimized to obtain accurate results for short interparticle distances, is nearly identical to $\psi_{CI-J}$ in the vicinity of the reference electron but underestimates the long-wavelength polarization of the atom, obtaining about 70% of the PCF of $\psi_{CI-J}$ on the other side of the atom. The mixing coefficient $\eta_1$ for the excited-state configuration was reduced by about 60% when the Jastrow factor was added to the multiconfiguration result, indicating that part of the polarization of the atom produced by the simple two configuration wavefunction is already accounted for by the Jastrow factor. In each case the $z$-axis PCF leads to a much larger peak on the far side of the atom than the $x$-axis case.

### C. Error Analysis

There are three sources of error in our calculation: statistical error in taking Monte Carlo estimates, the finite plane-wave cutoff of the data, and finally the variational bias due to the discrepancies of the trial from the true ground state wavefunction. The first two are closely connected and to some extent can be regulated; the third is harder to assess.

In a typical Monte Carlo calculation, sample points for evaluating the density or other single-particle expectation in a given region of space are generated with frequency proportional to the density itself. This leads to statistically precise measurements of the density at high density and large relative errors that vary roughly as $1/\sqrt{n(r)}$ at the vanishingly low densities outside the atom. Calculating the VMC expectations, $< \sum_i exp(-i\mathbf{G}\cdot\mathbf{r}_i) >$, of a set of plane-waves periodic on a supercell is equivalent to taking the Fourier transform of a histogram distribution of statistical sample points on that cell. The statistical outliers from the poorly sampled, asymptotic low-density region show up in the Fourier transform as a noise background independent of energy. This noise can to some degree be controlled by imposing a finite cutoff in reciprocal space. However, too small a cutoff leads to spurious long wavelength oscillations and is particularly poor for the short-distance region of the hole where the cusp condition results in a long range tail in the reciprocal space. We find that a good balance between controlling statistical and plane-wave error can be found by choosing a cutoff when the statistical average of the plane-wave component of the density is roughly equal to the statistical noise in its calculation. For a sampling size of around $10^5$ independent configurations, this cutoff limit proves to be about 32 Ry for a resolution of 1.0 $a_B$.

The statistical error of the Monte Carlo sampling was measured both for the individual plane-wave components of the density and conditional density, and for their real-space counterparts by measuring the standard deviation of these quantities over 10 to 20 independent runs. As shown in Fig. 3(c) and (d), the error bars of the PCF do in fact vary roughly as $1/\sqrt{n(r)}$ with well controlled errors in the peak density region, increasing to arbitrarily large values as one moves outside the atom. With the cutoff used, statistical errors in the PCF are limited to a value of less than 0.05 (out of a range in the PCF of the order of 1.0) for particles within 3.5 $a_B$ of the atom center, which in effect provides the limits in the plots of the PCF in Fig. 4.

The convergence of the plane-wave expansion was checked by plotting the PCF as a function of cutoff energy. A typical result is shown in Fig. 3(c) where the $x$-axis PCF for a particle fixed at 1.4 $a_B$ on the axis is plotted, for cutoff energies of 20, 28 and 32 Ry. The exact on-top hole has been measured by a direct VMC calculation and is plotted as a circle. The 20 Ry calculation shows clear deviations from the higher energy cutoff data, particularly in the region of the on-top hole, ie., in the immediate vicinity of the fixed electron, where the cusp condition contributes a high-energy tail to the exchange-correlation hole. The agreement between the two higher energy plots is well within statistical error except in the core region of the atom and in the low density tails. The

32 Ry case has not yet converged in the on-top region to the exact on-top value plotted as a circle, indicative of the slow convergence of the plane-wave expansion to the on-top hole cusp.

A final source of error is from the effect of the deviation of the variational trial wavefunctions [Eqs. (6) and (8)] from the exact ground state. The ground-state energy, being variationally optimized, is typically determined with much less error than other expectations (though one may expect that those important in the determination of the energy, such as the density and $n_{xc}$, should still be robust. An example of this problem is demonstrated in Fig. 4 in which two variationally optimized wavefunctions having relatively insignificant differences in total energy, give PCF's with noticeable differences for an electron fixed on the unoccupied $z$ axis. The variational method is in general more sensitive to errors in the wavefunction at high density as this region contributes the most to the variational energy. Thus we expect worse errors in the PCF when one or both coordinates are at low density.

In order to gauge possible errors arising from variational bias in our wavefunction, we study the change in the PCF and in $n_{xc}$ for several choices of trial wavefunction. Specifically we used trial wavefunctions with four, ten and eighteen Boys and Handy basis functions, corresponding to keeping expansion terms of order $o = l+m+n$ up to 2, 4 and 6 respectively in our Jastrow function. The lowest order function has, in addition to two terms that set the cusp condition for each spin component, only one electron-electron and one electron-nucleus term. The correlation energy of each wavefunction is 0.0640(8), 0.0812(4), and 0.0840(2) a.u. respectively, in comparison to 0.0877(2) a.u. using the multideterminant Slater-Jastrow wavefunction and 0.0883 a.u. for the CI calculation of Ref. [15].

In Fig. 5 we plot the opposite-spin PCF using these trial wavefunctions for two cases previously considered in Sec. IV: (a) an up-spin electron placed at 1.4 $a_B$ on the $x$ axis and (b) an up-spin electron placed at 4.0 $a_B$ on the $z$ axis. As in Fig. 3 we present a cut through the atom center and the reference electron, thus showing the minimum and maximum of the PCF. The first case represents a probable best-case situation, with the reference electron placed at peak density on an axis occupied by a $3p$ orbital, so that nondynamic correlations due to the open-shell structure should be neglible. In contrast the second case presents the worst case scenario: at low density along the unoccupied axis. The behavior of the PCF in the asymptotic low-density region of the atom is dominated by the statistical error of our plane-wave basis and is not shown.

In our best-case scenario, (a), the PCF near the reference electron is very well obtained with even the crudest model used ($o = 2$). On the far side of the atom with respect to the reference electron position, there is a noticeable increase in the magnitude of the peak of the PCF with the increase in accuracy of the wavefunction.

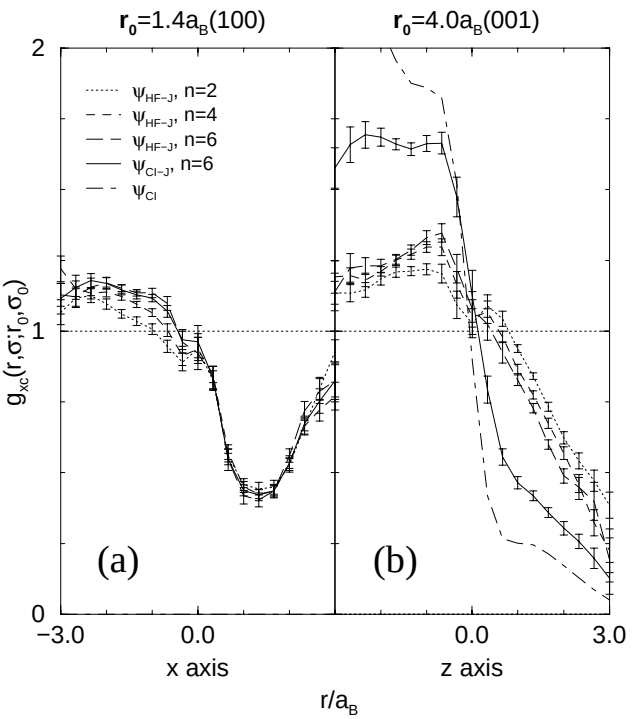


FIG. 5. Convergence data for the opposite-spin PCF for up-spin electron fixed at (a) 1.4 $a_B$ on the $x$ axis and (b) 4.0 $a_B$ on the $z$ axis. Cases shown are for Boys and Handy terms up to order $o = 2, 4,$ and 6 as described in the text, in a one-determinant Slater-Jastrow wavefunction, and $o = 6$ for a two-determinant Slater-Jastrow wavefunction. Additionally, results for a two-determinant wavefunction without Jastrow factor are given in (b) as a dot-dashed line.

As expected, the addition of nondynamic correlations in form of a two-determinant Slater-Jastrow wavefunction (solid line) has no noticeable effect. An investigation of the corresponding contour plots, cutting through the $x$-$z$ plane as shown in Fig. 4, shows that the depth and spatial extent of the PCF is obtained with the lowest order wavefunction and varies only slightly with increase in basis set. The major difference is the gradual adjustment of the $g = 1$ contour from a more isotropic shape to the elliptical one shown in Fig. 4(a), which accounts for the gradual increase in the peak on the far side of the $x$ axis as the $g = 1$ contour moves towards the atom center.

The worst case scenario (b) shows a far greater degree of disagreement between wavefunctions. The three one-determinant Slater-Jastrow wavefunctions agree fairly well with each other, with an increasing percentage of the electron density removed from the near side of the atom and placed on the far side. The peak height on the far side is roughly the same as for the 1.4 $a_B$, high-density case shown in Fig. 3(d). The introduction of the nondynamic $3s^2 \rightarrow 3p^2$ excitation into the Slater-Jastrow wavefunction (solid line) leads to a dramatic change in the shape of the PCF. The peak of the PCF from the base value of $g = 1$ representing no change due to correlations is increased by a factor of three, and only at the

on-top hole (not shown) is there no significant change in the PCF. In comparison, the PCF of the optimized two-determinant wavefunction $\psi_{CI}$ discussed in Sec. V is shown as a dot-dashed line. The two-determinant Slater-Jastrow wavefunction is an interpolation between the two limiting cases, favoring $\psi_{CI}$ at most locations.

An explanation of the "gigantic" features in the nondynamic part of the PCF in Fig. 5(b) comes from the observation that the ratio $zR_p(r)/R_s(r)$ between the $3p$ and $3s$ orbital, which determines the shape of the nondynamic PCF to first order [Eq. 12], increases exponentially at large distances along the $z$ axis. As a result, in the asymptotic region (that is, either the response to a reference electron outside the atom or the asymptotic tails of the response to a reference electron at high density), the nondynamic correlation introduced with the $3s^2 \rightarrow 3p_z^2$ substitution is no longer a small perturbation even with a small mixing parameter. The Jastrow factor basis functions however are chosen to tend to a constant at either large electron-electron or electron-nucleus distances. It is quite likely that none of the cases studied accurately represents the true asymptotic behavior of the correlation function. They should rather be considered to provide a qualitative idea of the PCF as well as a sense of the range of behavior it should reasonably lie within.

It is interesting to note that the agreement between the various PCF's is far closer for the high density case on the $z$ axis plotted in Fig. 3(d). This indicates the greater weight of the exchange-correlation hole at high density in determining the total exchange-correlation energy, and the corresponding robustness of its determination even with qualitatively different wavefunctions. Given the large degree of variation in the asymptotic limit, it would be interesting to study the effect of including a larger number of configurations in a multideterminantal Slater-Jastrow wavefunction or include the effects of backflow or multielectron coordinates [14] into the evaluation of orbitals. At higher densities we expect the effect of such improvements in the wavefunction would be to add further refinements in the shape of the PCF along the $z$ axis, but with much less change in basic features such as its range and magnitude.

## VI. CORRELATION EFFECTS ON THE SPIN DENSITY

In addition to the exchange-correlation hole, the spin components of the single-particle density change with the inclusion of Coulomb correlations. In principle, the Kohn-Sham equations used to derive the density in DFT should give the exact ground-state radial density, even for a degenerate ground-state [12]; however there is no such principle for the spin components of the density. Thus a change observed in the spin components of the density that does not alter the total radial density can be considered an intrinsic feature of Coulomb correlation and not simply due to the inaccuracy of the LDA density. As with $n_{xc}$, a prominent feature of the change in the spin-dependent density, $\Delta n(\mathbf{r}, \sigma)$, is anisotropy with respect to the fully occupied $x$ and open $z$ axes. This anisotropy in $\Delta n(\mathbf{r}, \sigma)$ may help to shed light on the mechanisms underlying the anisotropy in $n_{xc}$.

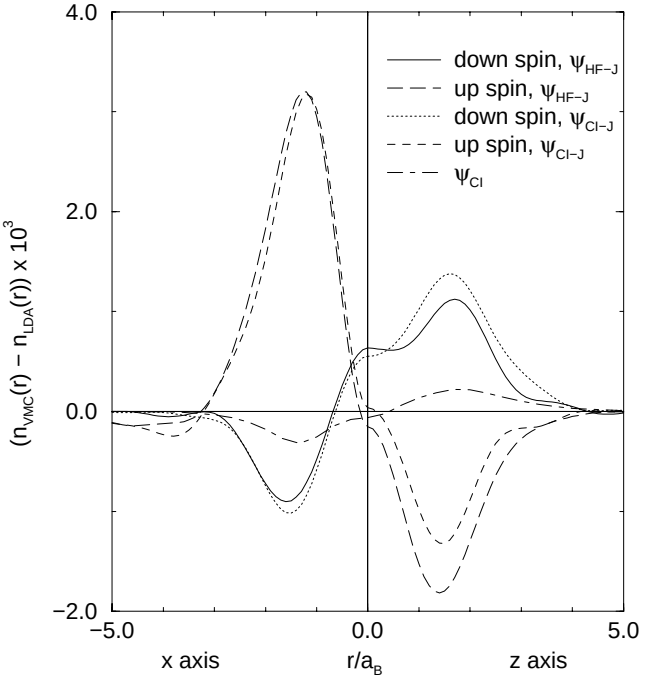


FIG. 6. The change in the spin-dependent density $n_1(\mathbf{r}, \sigma) - n_0(\mathbf{r}, \sigma)$ between the fully interacting and noninteracting systems. The left side of the plot shows a cut through the $x$ axis; the right side, through the $z$ axis. The solid line is the spin-down density change using the one-determinant Slater-Jastrow wavefunction $\psi_{S-J}$; the long-dashed is the spin-up density change for the same wavefunction. Dotted and dashed lines give the corresponding quantities for the two-determinant Slater-Jastrow function $\psi_{CI-J}$. The dot-dashed line is for the two-determinant function $\psi_{CI}$. The plot units are $10^{-3}$ a.u.

In Fig. 3, the spin-down density for the single determinant Slater-Jastrow wavefunction is plotted as a dotted line along the $x$ axis (a) and $z$ axis (b). Note that in the noninteracting wavefunction this density is that of the $3s$ orbital and thus the same along each axis. However, in the interacting case, anisotropy in the correlation response reduces the density along the $x$ axis by roughly 6% and increases it by the same amount along the $z$-axis. This change is shown in Fig. 6 (solid line) along with the change in the spin-up density (long-dashed line), with the right side of the plot showing a cut through the $x$ axis and the left side a cut through the $z$-axis. The corresponding density changes using the two-determinant Slater-Jastrow wavefunction ($\psi_{CI-J}$) are plotted as dotted and dashed lines. In both cases, the change in the spin-up density has a qualitative trend opposite to that of the spin-down density, showing a large enhancement

in density near the peak of the $3p_x$ orbital and a drop in density along the $z$ axis. Thus, the changes in the two spin components cancel out partially in the total density, but add to the total spin density, defined as $m(\mathbf{r}) = n(\mathbf{r},\uparrow) - n(\mathbf{r},\downarrow)$. In addition there are observable effects of a small reduction in the radius of the atom that occurs with the addition of the Jastrow correlation term, particularly a reduction in up-spin density at a large distance from the atom and an enhancement of the down-spin density in the core region. A convergence test along the lines of that for $n_{xc}$ in the previous section was carried out for the spin components of the density. The qualitative trends are repeatable with the less accurate Jastrow factors but with considerably slower quantitative convergence than for $n_{xc}$.

An anisotropic shift in spin density can be generated from the nondynamic Fermi correlation discussed in the previous sections: the mixing of the noninteracting ground-state with a $3s^2 \rightarrow 3p_z^2$-substitution excited state and the lack thereof due to Pauli exclusion for the $3p_x$ and $3p_y$ analogs. Using the two-determinant wavefunction $\psi_{CI}$, the resulting change in each spin component of the density is

$$\Delta n(\mathbf{r},\uparrow) = \Delta n(\mathbf{r},\downarrow) = \eta_1^2(|\psi_{3p_z}(\mathbf{r})|^2 - |\psi_{3s}(\mathbf{r})|^2) \quad (13)$$

where $\psi_{3s}$ and $\psi_{3p_z}$ are the wavefunctions of the $3s$ and $3p_z$ orbitals and $\eta_1$ the excited state probability amplitude. This function, shown as a dash-dotted line in Fig 6, corresponds to a density enhancement along the $z$ axis and reduction in the $x$-$y$ plane for *both* spin-components for a net zero change in the spin density $m(\mathbf{r})$, in marked contrast to the mutually opposing changes of the two spin-components of the Monte Carlo data. Given the optimal value of $\eta_1^2 = 0.017$ for the occupation number of the excited-state configuration, one finds that the magnitude of the change in either spin component of the density is much smaller than observed, and qualitatively in the wrong direction for the up-spin case. When the nondynamic $s^2 \rightarrow p_z^2$ excitation is included into the Slater-Jastrow wavefunction (dotted and dashed lines), both the up-spin and down-spin densities are enhanced slightly along the $z$ axis, but the qualitative picture remains unchanged – as one might expect from the very small value of $\eta_1^2 = 0.003$ that was optimal for this case. For these reasons, it is unlikely that the observed anisotropic change in the spin components of the density can be explained by this type of mechanism.

On the other hand, a simple explanation of these results lies in that the observed change in the spin density reduces the spatial overlap between the two spin components. As the correlation energy is predominantly determined by the spatial correlation between opposite-spin electrons, such a change in spin density can reduce the correlation energy in a way that reduces the total energy if the total density remains unchanged. This correlation effect is similar to that of the unrestricted Hartree-Fock method [37] in which the energy of a system like $H_2$ can be lowered from its Hartree-Fock value by breaking a symmetry of the ground state to induce the spatial separation of opposite spin-components of the density. In the Si atom, since the ground state is degenerate and lacks the symmetry of the Hamiltonian, it already has a nonzero spin density; multiplication by a Jastrow factor does not break the symmetry of the ground state in a substantial way [38]. The change in spin-density reflects the effect of the Coulomb interaction which induces the spatial separation between opposite spin electrons, in a system in which the different spin components are to some degree already spatially separated in the noninteracting state. In contrast to a filled-shell atom or other spin-unpolarized system, this spatial separation of opposite spins appears not only as a correlation hole but as a change in the mean density as well. Consistent with this picture, the direction of the change in the $L_z = 0$ projection of the Si atom enhances the absolute difference in the spin density $|n(\mathbf{r},\uparrow) - n(\mathbf{r},\downarrow)|$ that already exists in the Hartree-Fock wavefunction, where up-spin electrons occupies $p_x$ and $p_y$ orbitals while the lone down-spin electron does not.

## VII. SUMMARY AND CONCLUSION

We have calculated the exchange-correlation hole of the valence shell of the ground state of the Si atom as a function of spin decomposition, using the Variational Monte Carlo method. This relatively simple four electron system, restricted to a single valence shell, nevertheless shows a rich variety of phenomena in exchange and correlation not present in closed-shell atoms.

The incomplete filling of the valence shell of the open-shell atom leads to dramatic anisotropy and nonlocality in the exchange hole, even at peak densities in the valence shell. This is accompanied by a significant compensating anisotropy in the correlation hole making the total exchange-correlation hole more (but not completely) local and isotropic.

Our paper has focused mostly on the exchange-correlation hole about a majority (up) spin electron. In this case, as one goes from a reference point at peak density along an "occupied" axis, along which one of the occupied $3p$ orbitals is oriented, to one on the "open" $z$ axis perpendicular to the $3p$ orbitals, the exchange hole changes from an efficiently screening $3sp^2$-like to a poorly screening $3s$ character. As a result, we observe in the response of the minority (down) spin density a significant "dipole" shift or shift of density from one side of the atom to the other, that occurs when the up-spin electron is placed in the peak density position on the open axis and not when it is placed in the center of a $p$ orbital. This difference shows up in the pair correlation function as a difference in shape, with that on the "occupied" axis being a modest distortion of the isotropic shape of a dynamic correlation, and that on the $z$ axis showing a

marked dipole component along the $z$ axis. The dipole polarization observed is also notable in that it occurs not only for a reference electron outside the atom but at the peak along the $z$ axis, where the local gradient is zero; it is therefore a truly nonlocal feature not amenable to modeling by an expansion in the local density gradient.

The explicit inclusion of nondynamic correlations into our wavefunction enhances the difference between open and occupied-axis response, particularly when the reference electron is moved outside the atom. This is due to the exclusion effect in which the $3s^2 \rightarrow 3p^2$ substitution is allowed along the open axis and excluded along the occupied ones. Nevertheless, the existence of such a difference in the single-determinant Slater-Jastrow wavefunction, given the structure of the Jastrow factor, seems better explained in terms of the screening of the exchange hole, in which the Coulomb interaction of the down spin electron with the up-spin $3s$ exchange hole causes the dipole response along the open axis. In this case, it is the lowlying $3p$ orbital that best compensates for the poor screening of the exchange hole. It should thus play an important if not exclusive role in inducing the anisotropy of the opposite spin correlation hole.

A second major effect of the open-shell structure of the atom upon its response to the Coulomb interaction is the change of the spin components of the density with the addition of correlations. The down-spin density is pushed inwards and onto the unoccupied axis and the up-spin density pushed off the $z$ axis and onto the peak of the $p$ orbitals in the $x$-$y$ plane, resulting in a reduction of the spatial overlap between the two spin components in a way which leaves the radial density largely unchanged. The standard exclusion effect resulting from the $3s^2 \rightarrow 3p_z^2$ substitution produces a net change in density that is both quantitatively too small and qualitatively incorrect. However, both the anisotropic features of the exchange-correlation hole and the changes in spin density essentially stem from the same effect: the tendency of the Coulomb interaction to induce the spatial separation of opposite spin electrons in the context of the spatially anisotropic and spin-polarized structure of the degenerate Si ground state.

We have only briefly discussed the $n_{xc}$ for a down-spin electron, where in addition to the screening of the exchange hole (always $3s$-like), the anisotropy of the determinantal structure of the up-spin electrons plays an important role. The correlation response to the down-spin electron on the occupied axis combines a compensation for poor screening by the exchange hole and the absence of a lowlying $3p$-orbital component from the correlation hole on account of Pauli exclusion. We have observed in this situation subtle structural properties in the PCF that merit further investigation.

In contrast to longer ranged features of the correlation hole we find that its on-top value – the reduction of electron density in the immediate vicinity of an electron – is reproduced by a local density ansatz within 10-20%, over a fairly wide range in density and magnetization, and is otherwise insensitive to the structure of the atom. Given the energetically reasonable shape of the LDA $n_{xc}$ and that it satisfies the short-range cusp condition and global particle-sum rule of the true $n_{xc}$ in addition to the approximate fit to the Si on-top hole, it is reasonable to expect that it will provide a good approximation for the angle- or system-averaged $n_{xc}$, that is, after averaging out many of the subtle angle or position dependent features studied here [8]. Nevertheless, the complex spin-dependent phenomena observed in this paper point to the inherent difficulty of systematically improving on local or semilocal density functional theories in systems with nontrivial valence-shell structure, such as open shell atoms or multiply-bonded molecules.

Our results provide support for several recent hybrid approaches to DFT. The combination of a short ranged on-top hole that is fairly well modeled by local density functional theory and longer-ranged exchange and exclusion effects that are not indicates the usefulness of density functional schemes which include the on-top hole as a basic component [32] or involve the hybridization of short-ranged local or semilocal density functionals with a more accurate treatment of longer ranged correlations using RPA [36] or CI [12]. The tendency of the correlation hole to cancel out the anisotropy in the exchange hole, and increase the sensitivity of the exchange-correlation hole to electron position, along with the quality of the on-top hole in the LSD approximation, lends support to recent hybrid approaches [22] which mix the exact exchange hole with an local DFT approximation of the full-coupling constant exchange-correlation hole. These methods rely on the assumption that the full coupling constant limit of the integral in Eq. (4) is more likely to be amenable to approximation by the isotropic, localized $n_{xc}$ of the homogeneous electron gas than the noninteracting limit dominated by exchange. In the case of the open-shell atom exclusion effects quite effectively cancel out the gross anisotropy in the exchange hole caused by the open-shell structure, at least within the region of peak valence density.

On the other hand, the changes in spin-density that we observe indicate that a standard Hartree-Fock or restricted CI basis set may be a less desirable starting point for implementing hybrid DFT methods in spin-polarized systems than, for example, a generalized Hartree-Fock approach that would allow for anisotropic distortions in the spin density due to Coulomb correlations. Also, it seems possible that more could be done to obtain accurate correlation energies within the local spin-density approximation with the incorporation of projection specific information.

One of us (A. C. Cancio) would like to thank Kieron Burke for helpful discussions. This work was supported by Sandia National Laboratories contract AP-7094 and the Campus Laboratories Collaboration of the University of California.

[1] R. O. Jones and O. Gunnarson, Rev. Mod. Phys. **61**, 689 (1989).

[2] Warren E. Pickett and Jeremy Q. Broughton, Phys. Rev. B **48**, 14859 (1993-II).

[3] G. Ortiz and P. Ballone, Phys. Rev. B **50**, 1391 (1994).

[4] J. P. Perdew and Y. Wang, Phys. Rev. B **46**, 12947 (1992-II); J. P. Perdew, K. Burke and Wang, Phys. Rev. B **54**, 16533 (1996).

[5] C. A. Coulson and A. H. Neilson, Proc. Phys. Soc. **78**, 831 (1961).

[6] J. Sanders and K. E. Banyard, J. Chem Phys. **96**, 4536 (1992).

[7] M. A. Buijse and E. J. Baerends, in *Density Functional Theory of Molecules, Clusters and Solids* ed. D. E. Ellis, (Kluwer Academic, Dordrecht, 1995).

[8] M. Ernzerhof, J. P. Perdew and K. Burke, in *Density Functional Theory*, ed. R Nalewajski, (Springer-Verlag, Berlin, 1996).

[9] K. Burke, J. P. Perdew and M. Ernzerhof, J. Chem. Phys. **109**, 3760 (1998).

[10] M. Ernzerhof, K. Burke and J.P. Perdew, in "Recent Developments and Applications of Modern Density Functional Theory", ed. J.M. Seminario (Elsevier, 1996).

[11] O. Sinanoglu, Adv. Chem. Phys. **6**, 315 (1968).

[12] A. Savin, Int. J. Quantum Chem. Symp. **22**, 59 (1996); A. Savin, in "Recent Developments and Applications of Modern Density Functional Theory", ed. J.M. Seminario (Elsevier, 1996).

[13] C. J. Umrigar, K. G. Wilson, and J. W. Wilkins, Phys. Rev. Lett. **60**, 1719 (1988).

[14] K. E. Schmidt and J. W. Moskowitz, J. Chem. Phys. **93**, 4172 (1990).

[15] L. Mitáš, E. L. Shirley and D. M. Ceperley, J. Chem. Phys. **95** 3467, (1991); L. Mitáš in *Computer Simulation Studies in Condensed Matter Physics V*, ed. by D. P. Landau, K. K. Mon, and H. B. Schuttler (Springer Verlag, Berlin, 1993).

[16] J. C. Kimball, Phys. Rev. A **7**, 1648 (1973).

[17] S. Fahy, X. W. Wang and Steven G. Louie, Phys. Rev. Lett. **61**, 1631 (1988).

[18] Randolph Q. Hood et al., Phys. Rev. Lett., **78** 3350 (1997); Randall Q. Hood et al., Phys. Rev. B, **57** 8972 (1998).

[19] D. C. Langreth and J. P. Perdew, Solid State Commun. **17**, 1425 (1975).

[20] M. Levy, in "Recent Developments and Applications of Modern Density Functional Theory", ed. J.M. Seminario (Elsevier, 1996).

[21] O. Gunnarson, M. Jonson and B. I. Lundqvist, Phys. Rev. B **20**, 3136 (1979).

[22] A. D. Becke, J. Chem. Phys. **98**, 1372 (1993); A. D. Becke, J. Chem. Phys. **98**, 5648 (1993).

[23] J. P. Perdew, K. Burke and Y. Wang, Phys. Rev. B **54** 16533 (1996).

[24] A. J. Thakkar et al., Int. J. Quantum Chem. **26**, 157 (1984).

[25] The exchange hole of DFT is nearly identical with the Fermi hole commonly studied in quantum chemistry. However, the noninteracting ground-state in DFT and the corresponding single-particle orbitals are determined by the Kohn-Sham equation and in principle obtain the density of the exact ground state, while the Fermi hole is usually defined in terms of the Hartree-Fock ground state. Similarly, the correlation hole defined with respect to the full coupling constant exchange-correlation hole is the analog of the Coulomb hole of Ref. [5].

[26] D. R. Hamann, M. Schlüter and C. Chiang, Phys. Rev. Lett. **43**, 1494 (1979); G. B. Bachelet, D. R. Hamann and M. Schlüter, Phys. Rev. B **26**, 4199 (1982).

[27] N. C. Handy, J. Chem. Phys. **58**, 279 (1973).

[28] D. Ceperley and M. H. Kalos in *Monte Carlo Methods in Statistical Physics*, edited by K. Binder (Springer Verlag, Berlin 1979).

[29] M. Ernzerhof, K. Burke and J.P. Perdew, J. Chem. Phys. **105**, 2798 (1996).

[30] Note that this argument refers to a perspective complementary to that held elsewhere in this paper and in the literature. One measures the correlation hole at a fixed position in the atom in response to a reference electron somewhere else, and varies the position of the *reference* electron. The corresponding hole measured at the fixed position should be largest when the reference electron is moved on top it.

[31] J. P. Perdew, A. Savin, and K. Burke, Phys. Rev. A **51**, 4531 (1995).

[32] J. P. Perdew, M. Ernzerhof, K. Burke and A. Savin, Int. J. Quantum Chem. **61**, 197 (1997).

[33] H. Yasuhara, Solid State Commun. **11**, 1481 (1972).

[34] A. C. Cancio and C. Y. Fong, to be published.

[35] In principle one should be able to measure the importance of this configuration by a calculation of the overlap between it and the Slater-Jastrow ground state; the significantly different nodal structure of the two states makes a VMC calculation of this quantity unreliable in practice.

[36] D. C. Langreth and J. P. Perdew, Phys. Rev. B **21**, 5469 (1980).

[37] see, for example, Peter Fulde, *Electron Correlations in Molecules and Solids*, (Springer-Verlag, Berlin, 1991).

[38] Because of the different treatment of opposite and same-spin cusp conditions in the Jastrow factor of Slater-Jastrow wavefunctions, the total spin quantum number $S^2$ will in general not preserved (C. J. Huang, C. Filippi and C. J. Umrigar, J. Chem. Phys. **108** 8838, (1998).) Imposing a spin-independent cusp condition was observed to change the up-spin component of the density noticeably, but preserved fairly closely the degree and anisotropy of spatial separation between spin-components induced by correlations.